Conference paper

Meltem Akkulak, Yasemin Kaptan, Yasar Andelib Aydin* and Yuksel Avcibasi Guvenilir

Lipase mediated synthesis of polycaprolactone and its silica nanohybrid

https://doi.org/10.1515/pac-2018-1011

Abstract: In this study, rice husk ash (RHA) silanized with 3-glycidyloxypropyl trimethoxysilane was used as support material to immobilize *Candida antarctica* lipase B. The developed biocatalyst was then utilized in the ring opening polymerization (ROP) of ε-caprolactone and *in situ* development of PCL/Silica nanohybrid. The silanization degree of RHA was determined as 4 % (w) by thermal gravimetric analysis (TGA). Structural investigations and calculation of molecular weights of nanohybrids were realized by proton nuclear magnetic resonance (^{1}H NMR). Crystallinity was determined by differential scanning calorimetry (DSC) and X-ray diffraction (XRD). Scanning Electron Microscopy (SEM) was used for morphological observations. Accordingly, the PCL composition in the nanohybrid was determined as 4 %, approximately. Short chained amorphous PCL was synthesized with a number average molecular weight of 4400 g/mol and crystallinity degree of 23 %. In regards to these properties, synthesized PCL/RHA composite can find use biomedical applications.

Keywords: *Candida antarctica* lipase B; 3-glycidyloxypropyl trimethoxysilane; rice husk ash; POC-17; polycaprolactone.

Introduction

Polycaprolactone (PCL) is a biodegradable and biocompatible polymer that has been studied intensively in medical field, especially for controlled drug delivery and tissue engineering applications [1–3]. PCL can be synthesized via ring opening polymerization (ROP) of ε-caprolactone mediated by acidic, basic, ionic, coordination or enzymatic catalysts. The focus is driven towards enzymatic catalysis due to multiple considerations of which environmental sustainability, high regio- and enantio-selectivity and elimination of toxic metallic residues are only a few [1, 4, 5]. Due to their catalytic activity for ester synthesis or transesterification reactions in organic solvents, various lipases, particularly, *Candida antarctica* lipase B (CALB), is successfully used in free and immobilized forms [6]. In this process, enzyme immobilization is a key issue for protection of the enzyme activity against changing reaction conditions such as the solvent type, pH, temperature and monomer concentration. Immobilization of the enzyme can be realized by physical adsorption, covalent bonding or entrapment of the enzyme in a polymeric network [7]. Amongst all, physical adsorption in which enzymes are immobilized on a support material through mainly hydrophobic interactions is the most common [8, 9]. Likewise, the commercially available CALB, Novozyme® 435 is immobilized upon an acrylic resin by physical adsorption. Recent advances in the immobilization of lipases have shown that silica (Si) based supports either in the form of silica

Article note: A collection of papers presented at the 17th Polymers and Organic Chemistry (POC-17) conference held 4–7 June 2018 in Le Corum, Montpelier, France.

***Corresponding author: Yasar Andelib Aydin,** Marmara University, Chemical Engineering Department, Istanbul, Turkey, e-mail: yasar.aydin@marmara.edu.tr
Meltem Akkulak: Istanbul Technical University, Molecular Engineering Department, Istanbul, Turkey
Yasemin Kaptan and Yuksel Avcibasi Guvenilir: Istanbul Technical University, Chemical Engineering Department, Istanbul, Turkey

networks, aerogels or particles, provide increased stability, high catalytic activity and reusability for multifarious applications [7, 10, 11].

Rice husk ash (RHA) is generated by calcination of rice husks at 600–900 °C. The chemical composition is mainly 92–97 % amorphous silica (SiO_2) and it is characterized with large specific surface area due to many cracks and interconnected pores [12, 13]. As a by-product of rice industry, RHA is cheap and easily accessible. Consequently, it is considered to be a suitable support for enzyme immobilization [14]. Chemical functionality of RHA can be enhanced by surface modification with silanization agents, such as 3-aminopropyl triethoxysilane (3-APTES) [15, 16].

Pure polymer properties can be improved and special functionalities can be developed by formulation of polymer nanocomposites. Nanohybrids are synthesized by filling polymer matrix with inorganic fillers. In accordance with the efficiency of dispersion, the synergy between the polymer and nanofiller often leads to improved mechanical performance, thermal resistance, antibacterial and optical properties [17]. In particular, silica containing inorganic fillers were found to be promising in terms of dispersion and high degree of grafting [8, 18]. PCL/Silica composites have been prepared mainly via sol-gel reactions in the presence of an acidic or basic catalyst. Such composites were successfully involved in bone regeneration and tissue engineering applications [19].

The present work aimed at developing a new catalytic system composed of CALB immobilized upon silane treated RHA and exploiting the potential of this catalytic system in the *in situ* development of PCL/Silica nanohybrids. Immobilized enzyme was characterized for its hydrolytic activity and efficiency. Meanwhile, PCL and PCL/Si nanohybrid were characterized in terms of surface morphology and chemical structure via scanning electron microscopy (SEM), Fourier transform infrared spectroscopy (FTIR) and proton nuclear magnetic resonance spectroscopy (^{1}H-NMR), respectively. Thermal properties were determined by thermal gravimetric analysis (TGA) and differential scanning calorimetry (DSC). Both DSC and X-ray diffraction (XRD) were used for investigation of the crystal structure.

Materials and methods

Materials

Free CALB (Lipozyme®, Sigma-Aldrich) was immobilized on surface-modified RHA. Rice husks were kindly supplied by a local rice production facility (Edirne, Turkey) and treated as described previously to obtain RHA [1]. 3-Glycidyloxypropyl trimethoxysilane (3-GPTMS, Acros) was involved in experiments as the silanization agent.

ε-caprolactone (99 %, $C_6H_{10}O_2$, Alfa Aesar), was used as monomer in polymerization reaction. Toluene (99 %, $C_6H_5CH_3$, Merck), chloroform (99 %, $CHCl_3$, Sigma-Aldrich) and methanol (99 %, CH_3OH, Merck) were utilized as solvents in various steps of polymerization and fractionation.

Surface modification of RHA

Surface modification was realized according to the procedure described as follows: 250 mg of RHA was mixed with 5 ml acetone and 750 µl 15 % (v/v) 3-GPTMS. The mixture was incubated in a water bath at 50 °C and shaken at 160 rpm for 2 h. Surface-modified RHA was filtered and washed with fresh toluene for three successive cycles. Finally, the filtrates were dried in an oven at 60 °C for 4 h. By this procedure, epoxy ring-ended RHA was obtained.

Enzyme immobilization

Free CALB was mixed with 250 mg of surface-modified RHA in enzyme to support ratio of 2 µl · mg^{-1}. The reaction was conducted in 25 ml of 0.015 M phosphate buffer solution (pH 7.0) for 5 h at room temperature. After

successive washings with buffer solution, immobilized enzyme was filtered and dried at 30 °C. Immobilized CALB was then stored at 4 °C until use. The activity of the immobilized CALB and the immobilization efficiency were assayed by the methods described previously [15].

Development of RHA/silica nanohybrid systems

Immobilized CALB was utilized in the ROP of ε-caprolactone and development of nanohybrid systems. The polymerization reaction was conducted in toluene medium with monomer to enzyme ratio of 5 (w:w) at 40 °C. After 48 h, chloroform was added to terminate polymerization. Reaction product consisting of PCL and PCL/RHA hybrid system was precipitated with methanol. In order to prove the actual grafting of PCL upon RHA, the reaction product was fractionated by three successive chloroform washing and centrifugation cycles so as to obtain PCL rich and RHA rich phases. Both samples were oven dried at 35 °C.

In later experiments, fractionation step was omitted and thus, a composite of PCL and PCL/RHA was produced. The product was dried under similar conditions and kept in desiccator until being characterized. Reusability of the lipase immobilized upon RHA was investigated through four successive polymerization cycles. Accordingly, immobilized lipase was filtrated from the reaction mixture at the end of polymerization and washed with phosphate buffer (pH 7, 0.015 M). After being dried in oven at 30 °C, the enzyme was re-utilized for polymerization under the experimental conditions described previously in this section. The molecular weight of the synthesized polymer and monomer conversion were determined at the end of each cycle.

Characterization techniques

The effects of 3-GPTMS modification on the chemical and porous structure of RHA were determined by means of thermal gravimetric analysis (TGA), Fourier Transform Infrared Spectroscopy (FTIR) and N_2 adsorption. For thermogravimetry, sample sizes of 10–20 mg were heated to 900 °C with a rate of 10 °C/min under N_2 atmosphere using Seiko TG/DTA 6300 instrument. A NOVA 2200e BET instrument was used to characterize surface area and pore volume. FTIR spectra were recorded within the range 4000–650 cm^{-1} as an average of 32 scans at 2 cm^{-1} resolution (Perkin-Elmer, Spectrum One).

The RHA rich fraction was subjected to thermogravimetric analysis through the previously described procedure in order to determine the grafting efficiency of PCL onto RHA. The structure and molecular weights of the PCL/RHA composites were investigated by proton nuclear magnetic resonance (^{1}H-NMR). The ^{1}H-NMR spectra were recorded on Bruker Ultrashield 300 MHz apparatus after dissolving 10 mg of sample in 0.75 ml of deuterated chloroform in NMR tubes. The molecular weight (M_n) of PCL was calculated according to Eq. (1).

$$M_{n,\mathrm{NMR}} = \frac{5 \times I(4.07)}{2 \times I(3.65)} M_{\varepsilon\text{-}CL} \tag{1}$$

In this equation, $M_{\varepsilon\text{-}CL}$ represents the molecular weight of ε-caprolactone and $I_{4.07}$ and $I_{3.65}$ are the integrated areas of characteristic peaks at 4.07 ppm (CH_2O) and 3.65 ppm (CH_2OH), respectively [20].

Differential scanning calorimetry (DSC) was used to determine the glass transition temperature (T_g), melting temperature (T_m) and fusion enthalpy (ΔH_f) of products. Characterization was conveyed using Seiko 7020 DSC instrument operated between −80 and 100 °C at 10 °C/min steps. Crystallinity percentage was calculated with Eq. (2):

$$X_C(\%) = \frac{\Delta H_{f,\mathrm{sample}}}{\Delta H_f} \times 100 \tag{2}$$

where, $\Delta H_{f,\text{sample}}$ and ΔH_f represent the fusion enthalpy of the synthesized product and theoretical value for 100 % crystal PCL (i.e. 139.3 J/g), respectively [21].

Crystal structure and crystallinity were also investigated by X-ray diffraction (XRD) analysis (PANalytical, XPERT PRO). The analysis was performed between $2\theta = 15–40°$ at 0.002° angular intervals.

Surface morphology of PCL/silica nanohybrid was viewed under scanning electron microscopy (SEM, JEOL JSM-6390LV). Accordingly, samples coated with platinum were observed at different magnifications under 5 kV.

Results and discussion

Modification of RHA and its effects on enzyme immobilization

The thermogram of 3-GPTMS modified RHA is shown in Fig. 1. Accordingly, the cumulative weight loss of modified RHA was found to be 5.47 %. A comparison of this value with that of raw RHA [22] revealed 3.72 % difference which was assigned as the 3-GPTMS fraction. Based on the composition of raw RHA [22] and silanization degree, the average molecular weight of 3-GPTMS modified RHA was calculated as 162.4 g/mol, approximately.

SEM images of raw and silanized RHA samples (Fig. 2) proved the success of surface modification with 3-GPMTS. The impurities originally present in rice husk, i.e. sands and rice husk powders, are the possible causes of exterior impurities observed in the surface of raw RHA (Fig. 2a) [12]. Meanwhile, due to the increased content of silica, much smoother surface morphology was observed for silanized RHA (Fig. 2b).

As a consequence of the structural changes, the specific surface area and porosity of RHA was significantly increased as listed in Table 1.

The surface area of RHA was increased by nearly 80 % after silanization, which is mainly a consequence of increased porosity and certainly in favor of immobilization efficiency. It was speculated that the decrease in average pore size from 14.26 nm to 9.60 nm would not hinder the immobilization of CALB on modified RHA due to the reported average particle size of 6.9 nm × 5.05 nm × 8.67 nm by Blanco et al. [23].

The immobilization of CALB upon modified RHA occurs mainly through the chemical reactivity between the amino, thiol and hydroxyl functionalities of the enzyme with epoxy groups [24]. The incorporation of epoxy ring of 3-GPTMS to RHA structure was verified by the occurrence of respective peaks in FTIR spectrum of modified RHA. The effects of CALB immobilization were also observable in the spectrum of CALB-modified RHA complex (Fig. 3).

The FTIR spectrum of 3-GPTMS involves characteristic peaks in 600–1600 cm^{-1} region [25], which are common with RHA structure. For instance, the spectral band observed in the 800–900 cm^{-1} region, associated with epoxy ring of 3-GPTMS by means of C–O torsion and C–C stretching vibrations [25], is also characteristic for Si–CH_3 rocking and Si–O stretching vibrations of RHA. Similarly, the overlapping broad band within 1050–1250 cm^{-1} region is assigned to Si–O–Si asymmetric stretching vibrations of RHA as well as to the C–H rocking and C–C stretching vibrations of epoxy ring of 3-GPTMS. Consequently, both the increase in the intensity and the narrowing of these bands were accepted as clear indications the incorporation of 3-GPTMS to RHA structure. The presence of CALB upon silanized RHA was verified by the presence of minor peaks observed at 1650 cm^{-1} and within 3250–3300 cm^{-1}. These peaks were related to the C=O stretching, NH_2 deformation and –OH stretching vibrations of carboxylic acids [11].

Immobilization efficiency, calculated on basis of protein assay, and relative activity determined with respect to the hydrolytic activity of the free enzyme are tabulated in Table 2. The specific activity of Novozyme 435® was also provided for comparative purposes.

Despite the weak absorbencies of the corresponding peaks in FTIR spectrum, respectively high hydrolytic activity of the synthesized catalytic system (i.e. 2030 U) provided solid proof of CALB presence on 3-GPTMS modified RHA. Moreover, the specific activity of the catalytic system was increased by 1.8 and 4 folds compared

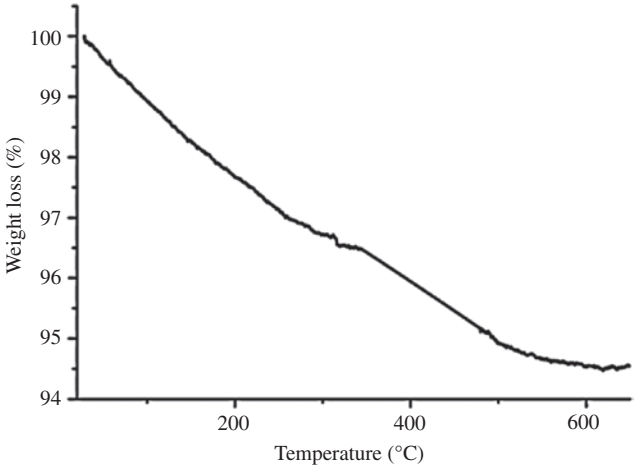

Fig. 1: The thermogravimetric curve of 3-GPTMS modified RHA.

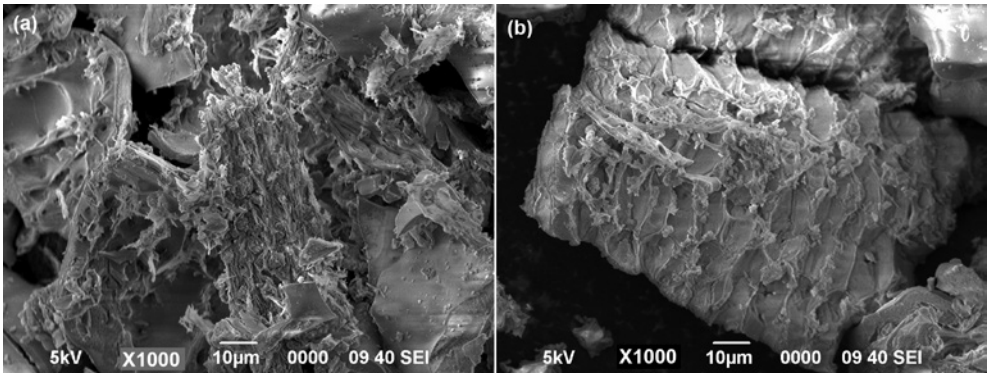

Fig. 2: SEM images of (a) raw RHA, (b) 3-GPTMS modified RHA.

Table 1: The surface area and pore size of RHA samples.

	RHA	3-GPTMS modified RHA
Surface area ($m^2 \cdot g^{-1}$)	50.61	90.28
Cumulative pore volume ($cm^3 \cdot g^{-1}$)	0.20	0.26
Average pore diameter (nm)	14.26	9.60

to Novozyme 435® and free lipase, respectively. Similar increments were also reported for CALB immobilized on epoxy functionalized support materials, previously [26]. Hyperactivation of CALB could be attributed to the ease of the access of substrate molecules to the active sites of the enzyme as a result of conformational changes [11, 26]. This phenomenon, also known as interfacial activation, is described as the opening of the active sites as a result of the interaction with hydrophobic support [6].

PCL grafting efficiency

The thermogravimetric analysis of RHA rich fraction (Fig. 4a) provided data for PCL grafting upon silanized RHA. Accordingly, the cumulative weight loss between 30 and 500 °C was higher for PCL/RHA composite due

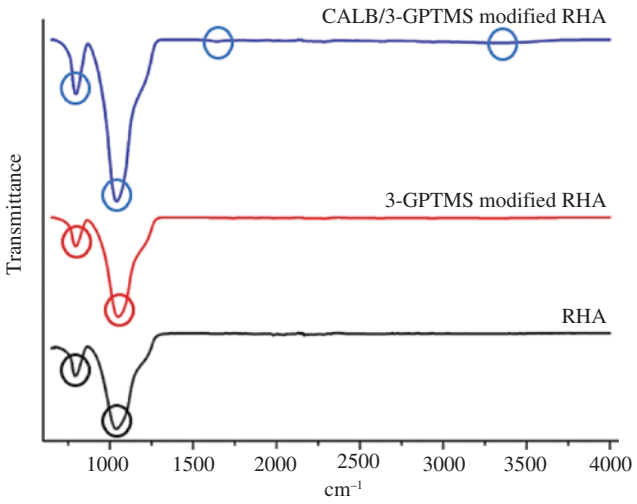

Fig. 3: FT-IR spectra of RHA, silanized RHA and the catalytic system.

Table 2: Hydrolytic activity of CALB immobilized upon 3-GPTMS modified RHA.

	Immobilization efficiency (%)	Activity (U)	Relative activity (%)	Specific activity (U · mg⁻¹)
Free lipase	–	2600	100	4.5
CALB/3-GPTMS modified RHA	88	2030	78	18
Novozyme 435®	n.d.	n.d.	n.d.	10

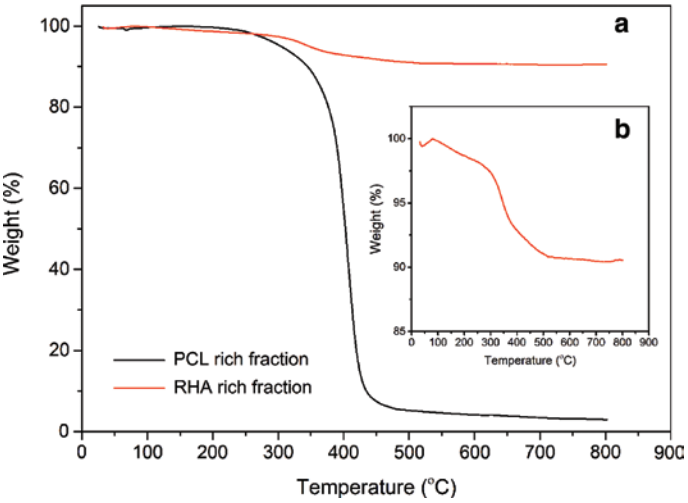

Fig. 4: TGA curves for (a) RHA rich fraction and PCL rich fraction. (b) Enlarged curve for RHA rich fraction.

to the increase in organic constituent. Thus, the difference between the cumulative weight losses of PCL/RHA composite and silanized RHA corresponded to the PCL grafting on silanized RHA.

Weight loss of silanized RHA was previously assigned as 5.47 %. Extraction of this value from that of RHA rich fraction leads to 3.96 %, which was determined as the amount of PCL grafting. Furthermore, PCL/RHA composite was distinguished from silanized RHA (Fig. 1) and PCL rich fraction in its thermal

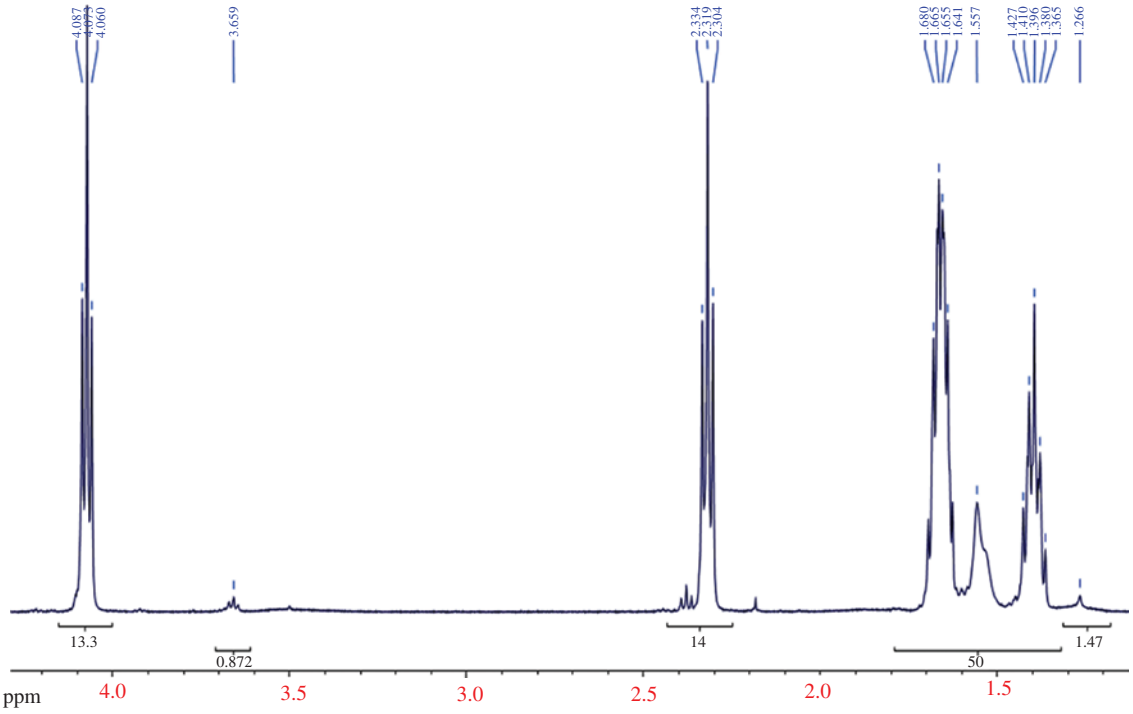

Fig. 5: ^{1}H-NMR spectra for PCL/silica nanohybrid.

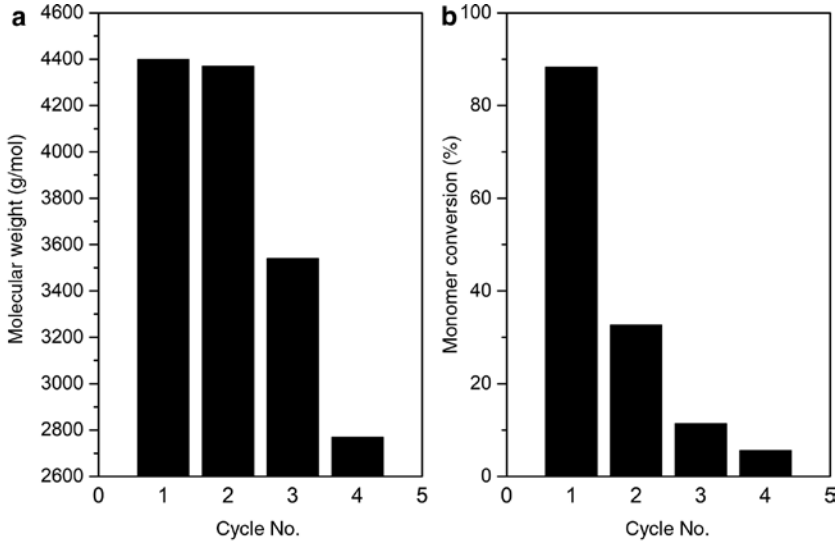

Fig. 6: Operational stability of CALB immobilized upon 3-GPTMS modified RHA in multiple polymerization cycles. (a) Molecular weight of nanohybrid, (b) monomer conversion.

degradation behavior. As clearly observed, the degradation of PCL/RHA composite involved two consecutive weight loss zones ascribed to 3-GPTMS and PCL constituents. Meanwhile, the degradation of PCL rich fraction was typical with a main degradation step within 400–450 °C [10]. The ambiguity in the initial part of TGA curve of PCL/RHA composite is neither due to PCL nor silanized RHA, but rather representative of an artefact since the mass loss which occurred in the range 32–50 °C was completely recovered with continued heating up to 79 °C, approximately.

Structural analysis of PCL/silica nanohybrids

Further structural characterizations were conducted for non-fractionated samples, i.e. *in situ* developed PCL/silica nanohybrids. The chemical structure of PCL and its molecular weight were exposed by ^{1}H-NMR analysis and corresponding spectra is shown in Fig. 5.

According to this figure, characteristic peaks of PCL at 4.07 (t, CH_2O), 3.65 (CH_2OH, end group), 2.30 (t, CH_2CO), 1.6–1.7 ($2\times CH_2$) and 1.2–1.37 (m, CH_2) ppm were present. Peak areas at chemical shifts 4.07 and 3.65 ppm obtained from ^{1}H-NMR spectra were substituted in Eq. (1) and according to the results, $M_{n,\mathrm{NMR}}$ was found as 4400 g/mol, approximately. Despite the high activity of the catalytic system, small PCL chains were synthesized. Previous investigations by Öztürk-Düşkünkorur et al. have suggested an inverse relationship between PCL chain length and the number of surface Si–OH groups. Similar output obtained in this study, support the proposed action of silanol groups as co-initiators for polymerization reaction resulting with high number of growing chains [8].

The results recorded upon repeated catalysis are presented in Fig. 6. Accordingly, upon repetitive utilization of the catalytic system, drastic reductions were recorded even by the second cycle for monomer conversion indicating loss in the number of active catalytic sites. Meanwhile, the molecular weight of PCL chains were relatively similar.

DSC curve and diffraction pattern of PCL/silica nanohybrid are provided in Fig. 7a,b. Based on the DSC scan (Fig. 7a), T_m and ΔH_f values were determined as 54 °C and 31.44 J/g, respectively. As compared to pure

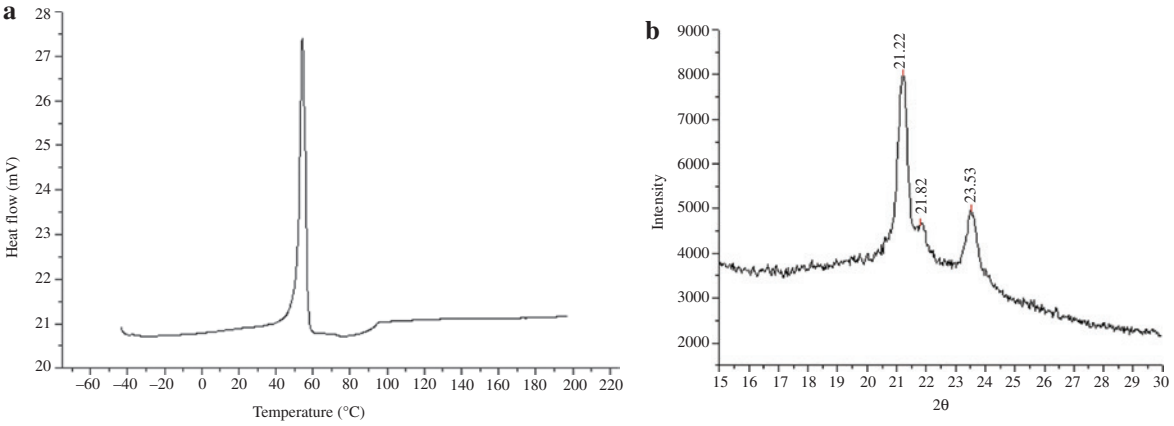

Fig. 7: Analysis of the crystal structure of PCL/silica nanohybrid, (a) DSC curve (b) X-ray diffraction pattern.

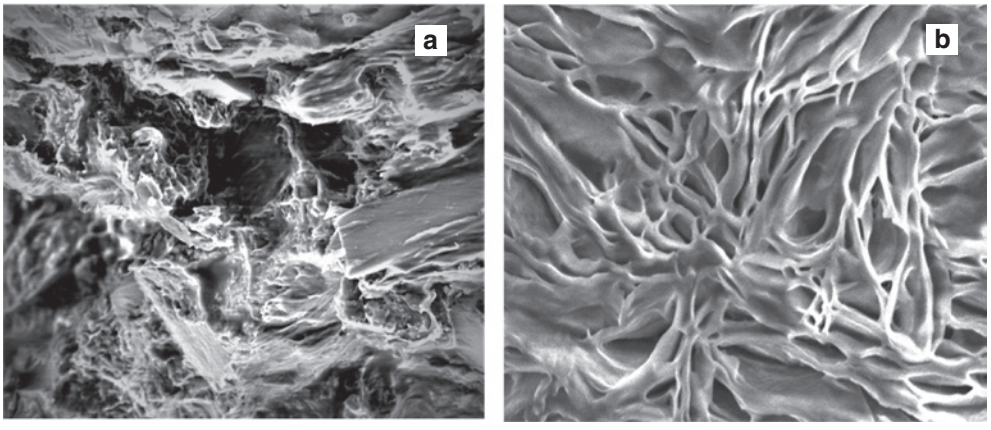

Fig. 8: SEM images of (a) PCL rich phase and (b) PCL/RHA nanohybrid.

PCL properties (data not shown), decrease of peak melting temperature from 60 °C to 54 °C, and crystallinity percentage from 65 % to 23 % was recorded. This could be related to the low molecular weight of PCL in the composite, which is known to affect the physical, thermal, mechanical properties and degradation rate of PCL, immensely [5]. An unexpected T_g of 93 °C observed in the DSC curve was a consequence of RHA presence.

The XRD pattern of the PCL/nanohybrid (Fig. 7b) presented the characteristics of semi-crystalline RHA and amorphous PLA with rather broad peaks of SiO_2 positioned at $2\theta = 21.22°$ and 21.82° corresponding to (101) lattice plane [12].

Surface morphology of the nanohybrid was unambiguously distinguished from PCL rich fraction (Fig. 8a,b) and silanized RHA (Fig. 2b). Despite the foam like structure of PCL rich fraction, the surface of PCL/silica nanohybrid was grainy. This implied that polymer chains growing from the silanized RHA coated the surface.

Conclusion

Hereby, RHA silanized by 3-GPTMS was used as carrier for *Candida antarctica* lipase B and the derived catalytic system was used in the ring opening polymerization of ε-caprolactone. The catalytic system offered an environmentally friendly route for *in situ* development of PCL/RHA hybrid system. The thorough characterization of the nanohybrid revealed that relatively short-chained PCL was synthesized up to a weight fraction of 4 %, approximately. The amorphous structure of the composite would certainly add limitations in terms of end uses, yet can be effectively used in biomedical applications like drug delivery. Further enhancements in PCL loading, molecular weight and crystallinity of the composite can be attained by optimization of process parameters such as monomer concentration, enzyme loading and polymerization time, which will be the scope of further research.

References

[1] C. Ulker, N. Gokalp, Y. Avcibasi-Guvenilir. *Adv. Mater. Lett.* **7**, 54 (2016).
[2] M. Labet, W. Thielemans. *Chem. Soc. Rev.* **38**, 3484 (2009).
[3] A. A. A. De Queiroz, É. J. França, G. A. Abraham, J. S. Román. *J. Polym. Sci. Polym. Phys.* **40**, 714 (2002).
[4] S. Kobayashi. *Macromol. Rapid. Commun.* **30**, 237 (2009).
[5] H. Pakalapati, A. B. Balaji, S. K. Arumugasamy, M. Khalid. *Polym. Bull.* **75**, 3227 (2018).
[6] P. Adlercreutz. *Chem. Soc. Rev.* **42**, 6406 (2013).
[7] J. Zdarta, A. S. Meyer, T. Jesionowski, M. Pinelo. *Catalysts* **8**, 92 (2018).
[8] H. Öztürk-Düşkünkorur, E. Pollet, V. Phalip, Y. Güvenilir, L. Avérous. *Polymers* **55**, 1648 (2014).
[9] R. A. Sheldon. *Adv. Synth. Catal.* **349**, 1289 (2007).
[10] D. Cazaban, L. Wilson, L. Betancor. *Curr. Org. Chem.* **21**, 96 (2017).
[11] J. Zdarta, L. Klapiszewski, A. Jedrzak, M. Nowicki, D. Moszynski, T. Jesionowski. *Catalysts* **7**, 14 (2017).
[12] J. Shen, X. Liu, S. Zhu, H. Zhang, J. Tan. *Mater. Lett.* **65**, 1179 (2011).
[13] X. Liu, X. Chen, L. Yang, H. Chen, Y. Tian, Z. Wang. *Res. Chem. Intermed.* **42**, 893 (2016).
[14] V. P. Della, I. Kühn, D. Hotza. *Mater. Lett.* **57**, 818 (2002).
[15] C. Ulker, N. Gokalp, Y. Guvenilir. *Biocatal. Biotransform.* **34**, 172, (2016).
[16] Y. Kaptan. M.Sc. Thesis, ITU, Institute of Science and Technology, Istanbul (2016).
[17] Y. Alonso, R. E. Martini, A. Iannoni, A. Terenzi, J. M. Kenny, S. E. Barbos, *Polym. Eng. Sci.* **55**, 1096 (2015).
[18] O. Monticelli, M. Calabrese, L. Gardella, A. Fina, E. Gioffredi. *Eur. Polym. J.* **58**, 69 (2014).
[19] C. E. P. Bonilla, S. Trujillo, B. Demirdögen, J. E. Perilla, Y. M. Elcin, J. L. G. Ribelles. *Mater. Sci. Eng. C* **40**, 418 (2014).
[20] N. Gokalp, C. Ulker, Y. Avcibasi-Guvenilir. *Adv. Mater. Lett.* **7**, 144 (2016).
[21] K. L. Harrison, M. J. Jenkins. *Polym. Int.* **53**, 1298 (2004).
[22] C. Öney-Kıroğlu, M.Sc. Thesis, ITU, Institute of Science and Technology, Istanbul (2014).
[23] R. M. Blanco, P. Terreros, M. Fernández-Pérez, C. Otero, G. Díaz-González. *J. Mol. Catal. B: Enzym.* **30**, 83, (2004).
[24] Q. Zhang, R. F. Huang, L. H. Guo. *Chin. Sci. Bull.* **54**, 2620 (2009).
[25] R. R. Silva, D. T. B. Salvi, M. V. Santos, H. S. Barud, L. F. Marques, S. H. Santagneli, A. Tercjak, S. J. L. Ribeiro. *J. Sol-Gel. Sci. Technol.* **81**, 114 (2017).
[26] S. P. de Souza, R. A. D. de Almeida, G. G. Garcia, R. A. C. Leão, J. Bassut, R. O. M. A. de Souza, I. Itabaiana, Jr. *J. Chem. Technol. Biotechnol.* **93**, 105 (2017).